# Isotopic Studies, Structure and Modeling of the Nitrous Oxide−Acetylene Complex

**Rebecca A. Peebles, Sean A. Peebles, and Robert L. Kuczkowski***

*University of Michigan, Department of Chemistry, 930 N. University Ave., Ann Arbor, Michigan 48109-1055*

**Helen O. Leung***

*Mount Holyoke College, Department of Chemistry, South Hadley, Massachusetts 01075*

*Received: July 29, 1999; In Final Form: October 11, 1999*

The microwave spectra of six isotopomers of HCCH·$N_2O$ have been measured. The structure of the complex has been fully determined. The monomers have a planar, nearly parallel orientation. They deviate from parallel by 13.6°, and the tilt moves the oxygen end of the $N_2O$ closer to the acetylene. The centers of mass of the two monomers are separated by 3.2961(8) Å. The dipole moment of the HCCH·$^{15}N_2O$ isotope has been measured, giving $\mu_a = 0.0915(7)$ D, $\mu_b = 0.1503(19)$ D, and $\mu_{tot} = 0.1759(16)$ D. The conclusions of this work refine previous experimental and semiempirical studies. New semiempirical calculations using a different model agree well with the current results.

## Introduction

The study of weakly bound complexes has long been used to gain insight into the nature of the weak forces that are present when molecules interact. The results of structural studies using high-resolution spectroscopy help refine theoretical interaction models, identifying areas where they function well and where they seem to break down. In this study, we examine the HCCH·$N_2O$ system. This complex has previously been studied experimentally by several groups,[1−3] and a semiempirical interaction model has been used to investigate the structure.[1,4] These initial studies proposed a parallel structure with a line perpendicular to the two monomers connecting their centers of mass. The available data from one isotopic species was insensitive to detecting small deviations from a parallel configuration. This structure is similar to that of the isoelectronic HCCH·$CO_2$ complex, which has been studied experimentally and with the same interaction model that was applied to HCCH·$N_2O$.[4−6] A different interaction model has recently been helpful in modeling the HCCH·OCS,[7] HCCH$(OCS)_2$,[8] $CO_2$·OCS,[9] $(CO_2)_2$OCS,[9,10] $(OCS)_2CO_2$,[11] and $(CO_2)_2N_2O$[12] complexes, among others. It was noted in the HCCH·OCS study that this model predicted that the oxygen end of the $N_2O$ would tip about 10−15° toward the acetylene molecule in the HCCH·$N_2O$ complex.[7] Other complexes involving $N_2O$ have shown similar decreases in symmetry when compared to the corresponding $CO_2$ complexes. For example, $H_2O$·$CO_2$ has $C_{2v}$ symmetry, with the oxygen of $H_2O$ pointing toward the carbon of $CO_2$ in a T-shaped configuration.[13,14] $H_2O$·$N_2O$ also has a T-shaped structure, but the oxygen of the $N_2O$ is drawn toward one of the $H_2O$ hydrogens, causing a distortion of the T.[15]

The current work investigates the discrepancy between the two sets of HCCH·$N_2O$ calculations by studying various isotopomers of the complex. This allows a complete structural determination which was not possible with the previous data from only one isotope. In addition, the semiempirical model that was used for the current work is contrasted with the model that was used previously in an attempt to explain why the two sets of predictions are different.

## Experiment

The spectra of six isotopomers of the HCCH·$N_2O$ complex were measured in the 5.5−18.5 GHz range on the Balle−Flygare type Fourier transform microwave spectrometers[16] at Mount Holyoke College and the University of Michigan.[2,17−19] The $H^{12}C^{12}CH$·$^{14}N_2O$ and $H^{12}C^{12}CH$·$^{15}N^{14}NO$ isotopomers were measured at Mount Holyoke by expanding a mixture of 1% HCCH and 2% $N_2O$ in argon through a General Valve Series 9 nozzle. The backing pressure was 4−5 atm. Measurement of the $H^{12}C^{12}CH$·$^{14}N_2O$ spectrum has been reported previously.[2] Spectra of the remaining four isotopomers, $H^{12}C^{12}CH$·$^{15}N_2O$, $H^{13}C^{12}CH$·$^{15}N_2O$, $H^{12}C^{13}CH$·$^{15}N_2O$, and $H^{12}C^{12}CD$·$^{15}N_2O$ were measured at the University of Michigan with a sample concentration of about 1% each of HCCH and $N_2O$ in argon with a stagnation pressure of 2−3 atm. A modified Bosch fuel injector valve was used. All of the isotopic species were measured using enriched samples. $^{15}N_2O$ (99% $^{15}N$) was obtained from Isotec; $H^{12}C^{13}CH$ (99.2% $^{13}C$) was obtained from CDN Isotopes; HCCD (98.9% D) was obtained from CDN, and $^{15}N^{14}NO$ (98% $^{15}N$) was obtained from Cambridge Isotopes. The Mount Holyoke nozzle was aligned parallel to the direction of microwave propagation, while the Michigan nozzle was perpendicular to the direction of microwave propagation, except for the HCCD·$^{15}N_2O$ isotopomer, for which a parallel arrangement was used. This alignment improves resolution, facilitating the assignment of nuclear quadrupole hyperfine structure, while the perpendicular nozzle arrangement eliminates Doppler doublets. Line widths from the parallel nozzle were 6−7 kHz full width at half-maximum (fwhm), while the perpendicular nozzle gave fwhm values of about 30 kHz. A typical transition of the normal isotopomer required 10 000 gas pulses to obtain a reasonable signal-to-noise ratio. Transitions of the $^{15}N_2O$ isotopomers were much stronger due to the lack of hyperfine structure. 200 shots were required to give a signal-to-noise ratio of about 20 for the b-type transitions of the $H^{12}C^{12}CH$·$^{15}N_2O$ isotopomer. Since two isotopic species were present in the

* Corresponding author.

10.1021/jp992672l CCC: $18.00 
Published on Web 11/12/1999

**TABLE 1: Spectroscopic Constants for HCCH·$N_2O$ and the Five Assigned Isotopomers (in MHz Unless Otherwise Noted)**

| | $H^{12}C^{12}CH\cdot{}^{14}N_2O$[a] | $H^{12}C^{12}CH\cdot{}^{15}N_2O$ | $H^{13}C^{12}CH\cdot{}^{15}N_2O$ | $H^{12}C^{13}CH\cdot{}^{15}N_2O$ | $H^{12}C^{12}CH\cdot{}^{15}N^{14}NO$[f] | $H^{12}C^{12}CD\cdot{}^{15}N_2O$[g] |
|---|---|---|---|---|---|---|
| $A$ | 9394.26826(22) | 9153.3378(12) | 9097.5293(37) | 9095.9382(42) | 9153.47455(15) | 8739.4775(32) |
| $B$ | 2831.85640(8) | 2786.8284(7) | 2718.3913(18) | 2725.1120(20) | 2808.76903(6) | 2734.3984(15) |
| $C$ | 2168.07804(7) | 2128.7172(6) | 2089.6146(14) | 2089.4814(16) | 2141.50685(5) | 2075.3275(12) |
| $D_J$ | 0.012290(3) | 0.011778(17) | 0.011450(51) | 0.011325(58) | 0.0120267(15) | 0.011133(80) |
| $D_{JK}$ | 0.056768(40) | 0.05545(14) | 0.05217(45) | 0.05448(51) | 0.0558972(76) | 0.05672(42) |
| $D_K$ | *b* | *b* | *b* | *b* | −0.060972(39) | *b* |
| $d_1$ | −0.003365(2) | −0.003232(24) | −0.003135(36) | −0.003041(40) | −0.0033240(6) | −0.003092(12) |
| $d_2$ | −0.000727(10) | −0.00060(10) | −0.000727[e] | −0.000727[e] | −0.0007028(5) | −0.000727[e] |
| $N$[c] | 15 | 12 | 11 | 11 | 22 | 11 |
| $\Delta\nu_{rms}$/kHz[d] | 0.832 | 1.00 | 3.24 | 3.68 | 0.227 | 2.81 |

[a] Data from ref 2. Fit of 121 hyperfine components from 15 rotational transitions. [b] $D_K$ was fixed at zero, because it was not well determined. [c] $N$ = number of rotational transitions in the fit. [d] $\Delta\nu_{rms} = (\sum(\nu_{obs} - \nu_{calc})^2/N)^{1/2}$. [e] Fixed at value from normal isotopomer. [f] Fit of center frequencies of 22 rotational transitions. [g] Fit of center frequencies of 11 rotational transitions.

**TABLE 2: Transition Frequencies for Isotopomers Measured in This Work (in MHz)**

| | | HCCH·$^{15}N_2O$ | | $H^{13}C^{12}CH\cdot{}^{15}N_2O$ | | $H^{12}C^{13}CH\cdot{}^{15}N_2O$ | | $H^{12}C^{12}CH\cdot{}^{15}N^{14}NO$ | | $H^{12}C^{12}CD\cdot{}^{15}N_2O$ | |
|---|---|---|---|---|---|---|---|---|---|---|---|
| $J'_{Ka'Kc'}$ | $J''_{Ka''Kc''}$ | frequency | obsd − calcd | frequency | obsd − calcd | frequency | obsd − calcd | frequency | obsd − calcd | frequency | obsd − calcd |
| $1_{10}$ | $1_{01}$ | 7024.498 | 0.001 | 7011.793 | −0.005 | 7006.335 | −0.001 | 7011.904 | 0.000 | 6664.025 | 0.000 |
| $1_{11}$ | $0_{00}$ | 11281.909 | −0.001 | 11183.009 | 0.003 | 11185.280 | 0.003 | 11294.896 | 0.000 | 10814.661 | 0.002 |
| $2_{11}$ | $2_{02}$ | 7730.701 | 0.000 | 7689.034 | 0.000 | 7686.870 | 0.000 | 7728.733 | 0.000 | 7374.085 | −0.001 |
| $2_{12}$ | $1_{11}$ | 9172.487 | 0.002 | 8974.765 | 0.005 | 8993.067 | −0.006 | 9232.787 | 0.000 | 8959.903 | 0.006 |
| $2_{02}$ | $1_{01}$ | 9782.297 | 0.001 | 9562.873 | −0.004 | 9583.602 | −0.004 | 9850.269 | 0.000 | 9567.775 | −0.005 |
| $2_{11}$ | $1_{10}$ | 10488.498 | −0.002 | 10240.116 | 0.003 | 10264.148 | 0.008 | 10567.099 | 0.000 | 10277.838 | −0.002 |
| $2_{12}$ | $1_{01}$ | | | | | | | 15577.456 | 0.000 | | |
| $3_{03}$ | $2_{12}$ | 8796.857 | 0.000 | 8442.289 | −0.004 | 8483.026 | −0.001 | 8924.629 | 0.000 | 8827.699 | 0.003 |
| $3_{12}$ | $3_{03}$ | 8877.647 | 0.001 | 8786.076 | 0.002 | 8789.659 | −0.004 | 8894.217 | 0.000 | 8531.793 | 0.002 |
| $3_{13}$ | $2_{12}$ | 13728.994 | −0.001 | 13434.585 | −0.004 | 13461.795 | 0.002 | 13818.563 | 0.000 | 13408.450 | −0.002 |
| $3_{03}$ | $2_{02}$ | | | | | | | 14651.816 | 0.001 | | |
| $3_{22}$ | $2_{21}$ | | | | | | | 14848.255 | 0.000 | | |
| $3_{21}$ | $2_{20}$ | | | | | | | 15045.833 | 0.000 | | |
| $3_{12}$ | $2_{11}$ | | | | | | | 15817.300 | 0.001 | | |
| $3_{21}$ | $3_{12}$ | | | | | | | 18312.559 | 0.000 | | |
| $4_{13}$ | $4_{04}$ | 10557.737 | 0.000 | 11389.275 | −0.001 | 10401.829 | 0.001 | 10603.136 | 0.000 | 10233.450 | 0.000 |
| $4_{04}$ | $3_{13}$ | 14258.122 | 0.000 | 13786.249 | 0.003 | 13837.908 | 0.000 | 14421.345 | 0.000 | | |
| $4_{22}$ | $4_{13}$ | | | | | | | 17528.244 | 0.000 | | |
| $4_{14}$ | $3_{13}$ | | | | | | | 18370.793 | 0.000 | | |
| $5_{14}$ | $4_{23}$ | | | | | | | 9369.400 | 0.000 | | |
| $5_{14}$ | $5_{05}$ | 12862.317 | 0.000 | | | | | 12948.239 | 0.000 | 12570.811 | 0.000 |
| $5_{23}$ | $5_{14}$ | | | | | | | 16914.301 | 0.000 | | |

$H^{12}C^{13}CH$ sample mixture ($H^{13}C^{12}CH\cdot{}^{15}N_2O$ and $H^{12}C^{13}CH\cdot{}^{15}N_2O$), there was a decrease in signal intensity. The $H^{12}C^{13}CH$ transitions required about 1000 gas pulses to obtain a signal-to-noise ratio of around 5, and the HCCD transitions also had similar intensity. The HCCD·$^{15}N_2O$ isotopomer with D close to the oxygen was assigned. The isotopomer with the D at the nitrogen end of the $N_2O$ was weaker, presumably due to an isotope effect, and not assigned. The a-type transitions of all species were considerably weaker due to the very small a-component of the dipole moment.

Stark effect measurements were carried out on the University of Michigan spectrometer by applying voltages of up to ±7 kV to two parallel 50 cm × 50 cm steel mesh plates spaced about 30 cm apart and located just outside the Fabry−Perot cavity of the spectrometer. The electric field was calibrated by measuring the $J = 1 \leftarrow 0$ transition of OCS at 12 162.980 MHz and assuming an OCS dipole moment of 0.7152 D.[20]

## Results

**A. Spectra.** Spectral data for the HCCH·$N_2O$ complex and results based on an analysis of the nuclear quadrupole hyperfine structure of the normal species have been published previously.[2,3] For the normal isotopomer, six a-type and nine b-type transitions were measured, while four a-type and eight b-type transitions were measured for HCCH·$^{15}N_2O$, and four a-type and seven b-type transitions were measured for each of the $H^{12}C^{13}CH$ isotopomers and the HCCD isotopomer. Nine *a*-type and 13 *b*-type transitions were measured for HCCH·$^{15}N^{14}NO$. The spectra were fit to Watson's S-reduction Hamiltonian in the $I^r$ representation. The spectroscopic constants for all of the isotopomers are given in Table 1. For most of the isotopes, $D_K$ was not well determined, so it was fixed at a value of zero. For the $H^{13}C^{12}CH$ species and HCCD species, $d_2$ was not well determined, and it was fixed at the value of $d_2$ from the normal isotope. The nuclear quadrupole hyperfine structure of the normal species has been analyzed previously,[2] and the hyperfine structures of $H^{12}C^{12}CH\cdot{}^{15}N^{14}NO$ and $H^{12}C^{12}CD\cdot{}^{15}N_2O$ will be treated in future work. For the current study, center frequencies after preliminary analysis of the quadrupole splittings of the $H^{12}C^{12}CH\cdot{}^{15}N^{14}NO$ and $H^{12}C^{12}CD\cdot{}^{15}N_2O$ transitions were fit to obtain rotational constants. The frequencies of all of the transitions measured in the current study are given in Table 2, including the unsplit center frequencies for $H^{12}C^{12}CH\cdot{}^{15}N^{14}NO$ and $H^{12}C^{12}CD\cdot{}^{15}N_2O$. The transition frequencies of the normal isotopomer are given in ref 2.

**B. Dipole Moment.** The dipole moment of the HCCH·$^{15}N_2O$ isotopomer was measured. The small dipole moment components and small Stark coefficients combined to give very small shifts in the transition frequencies. At the largest fields, the shifts were about 200−300 kHz. Data were obtained on one compo-

**TABLE 3: Observed and Calculated Stark Coefficients for HCCH·$^{15}N_2O$**

| $J'_{Ka'Kc'}$ | $J''_{Ka''Kc''}$ | $\|M\|$ | observed[a] | calculated[a] |
|---|---|---|---|---|
| $2_{11}$ | $2_{02}$ | 2 | 0.585 | 0.569 |
| $3_{12}$ | $3_{03}$ | 3 | 0.394 | 0.409 |
| $2_{11}$ | $1_{10}$ | 1 | −0.901 | −0.889 |
| $2_{12}$ | $1_{11}$ | 1 | 0.900 | 0.906 |
| $2_{02}$ | $1_{01}$ | 1 | 0.317 | 0.304 |
| $1_{10}$ | $1_{01}$ | 1 | 1.247 | 1.252 |
| $1_{11}$ | $0_{00}$ | 0 | 0.250 | 0.272 |

[a] Units of $10^{-6}$ MHz cm$^2$ V$^{-2}$. The calculated coefficients were obtained with the constants in Table 1 and dipole components in Table 4.

nent each from seven transitions, and a least-squares fit of the measured Stark coefficients led to dipole moment components of $\mu_a = 0.0915(7)$ D and $\mu_b = 0.1503(19)$ D, with $\mu_{tot} = 0.1759(16)$ D. The dipole moment data are summarized in Tables 3 and 4. Projection of the $N_2O$ dipole moment (0.16083 D[21]) onto the principal axes of the complex predicts a pure b-type spectrum for HCCH·$N_2O$, since the $\mu_a$ projection is too small to be observed unless polarization effects increase it substantially. Hence, the presence of a-type transitions indicates that there is an induced dipole along the a-axis. Determination of a dipole moment with both a- and b-components confirms this. These results for HCCH·$N_2O$ are consistent with the results for the isoelectronic complex HCCH·$CO_2$, where the dipole moment of 0.161 D is due entirely to induction effects.[5] Calculations using a semiempirical model, described later, predict only the b-component of the dipole moment of HCCH·$N_2O$ when induction is omitted from the calculation, but when distributed polarizabilities are included an a-component close to the experimental value is predicted. These dipole moment results are summarized in Table 4 for comparison with experiment and will be analyzed further in the Discussion.

**C. Structure.** The spectra of the six assigned isotopic species provided 18 moments of inertia with which to determine three structural parameters. These parameters are the $N_2-M_4-M_9$ and $M_4-M_9-C_7$ angles and the $M_4-M_9$ (center of mass) distance, using the numbering scheme shown in Figure 1. The moments of inertia of the normal species lead to a planar moment ($P_{cc} = 0.5(I_a + I_b - I_c)$) of −0.421 amu Å$^2$. This small negative number indicates that the complex is planar and relatively rigid. A fit of the structural parameters to all of the moments of inertia leads to a large standard deviation because of the inertial defect, and for this reason, only $I_a$ and $I_b$ for each isotope were included in the inertial fit. This led to a structure determination with a $\Delta I_{rms}$ of 0.107 amu Å$^2$ and with $\theta_{N_2-M_4-M_9} = 93.9(5)°$, $\theta_{M_4-M_9-C_7} = 80.3(8)°$ and $r_{cm} = 3.2961(8)$ Å.[22] This is an effective ground-state structure, and $r_{cm}$ should be within 0.05 Å and the angles within 5° of the equilibrium values. The structural parameters are summarized in Table 5. It was assumed that the structures of the monomers would remain unchanged from their uncomplexed values ($r_{N-O} = 1.191$ Å, $r_{N-N} = 1.126$ Å[23] and $r_{C-H} = 1.061$ Å, $r_{C-C} = 1.203$ Å[24]).

The assignment of the new isotopic species allowed the determination of Kraitchman substitution coordinates for both of the nitrogen atoms, both of the carbon atoms and one hydrogen atom in the complex.[25] The absolute values of the Kraitchman coordinates are given in Table 6 which also shows the principal axis coordinates of the structure obtained from the inertial fit. The coordinates of atoms $H_8$, $C_6$, $C_7$, and $N_2$ were obtained by treating the $H^{13}C^{12}CH\cdot{}^{15}N_2O$, $H^{12}C^{13}CH\cdot{}^{15}N_2O$, $H^{12}C^{12}CH\cdot{}^{15}N^{14}NO$, and $H^{12}C^{12}CD\cdot{}^{15}N_2O$ species as single substitutions of the $H^{12}C^{12}CH\cdot{}^{15}N_2O$ isotope. The coordinates of atom $N_1$ were determined from $H^{12}C^{12}CH\cdot{}^{15}N^{14}NO$ and the normal isotopomer. The substitution coordinates are obtained in the principal axis system of the parent species, so it was necessary to transform the coordinates of atoms $N_2$, $C_6$, $C_7$, and $H_8$ to the principal axis system of normal HCCH·$N_2O$ before comparisons could be made. It is the transformed coordinates that are shown in Table 6. The only coordinate that differs significantly from the inertial fit coordinates is *a* for atom $N_1$. The substitution structure gives a value for this coordinate that deviates by 0.094 Å from the inertial fit.

A two-parameter fit holding the HCCH and $N_2O$ units parallel was also explored. In this fit, $r_{cm}$ and $\theta_{N_2-M_4-M_9}$ were varied holding $\theta_{M_4-M_9-C_7}$ equal to $\theta_{N_2-M_4-M_9}$ (see Figure 1). The best least-squares fit to $I_a$ and $I_b$ for the six isotopic species gave $r_{cm} = 3.29924(66)$ Å and $\theta_{N_2-M_4-M_9} = 84.35(23)°$. The quality of the fit ($\Delta I_{rms} = 0.132$ amu Å$^2$) was poorer than for the tilted structure fits. A comparison of the Cartesian coordinates from this fit and the Kraitchman coordinates is given in Table 6. Although the $\Delta I_{rms}$ is not substantially different for this structure, the Cartesian coordinates are in overall poorer agreement with the Kraitchman calculated values compared to the tilted configuration. This leads to our preference for the tilted structure as the best fit to the isotopic shift data. Still, the overall comparisons of $\Delta I_{rms}$ and the Kraitchman coordinates are not so unequivocally compelling that the parallel structure can be definitively eliminated. Large-amplitude vibrational effects on the moments of inertia contribute a residual ambiguity in the interpretation of the isotope shift data.

The substitution coordinates can be used to calculate the N−N and C−C distances and one C−H distance in $N_2O$ and HCCH. This calculation leads to an N−N distance of 1.144 Å, a C−C distance of 1.205 Å, and a C−H distance of 1.059 Å. These differ by about 0.02, 0.002, and 0.002 Å, respectively, from the monomer values. This is reasonable agreement given that large-amplitude effects on the rotational constants have not been taken into account.

## Discussion

The data from six isotopomers of HCCH·$N_2O$ have allowed a full determination of the structure of the complex. The inertial fit, supported by substitution coordinates for five atoms, indicates that the two molecules deviate from parallel by 13.6°. The oxygen of the $N_2O$ inclines toward the acetylene molecule. Semiempirical modeling using the ORIENT program,[26] which is described presently, gives structures in good agreement with these results.[7] This is in contrast to earlier studies of HCCH·$N_2O$ which proposed a parallel or nearly parallel structure.[1−3] These studies used a different semiempirical model, developed by Muenter, to model the HCCH·$N_2O$ system.[1,4] This model was in agreement with the parallel structure that had been proposed. The two semiempirical models differ in the form of the dispersion−repulsion terms that are used and also in the distributed multipole moments which were employed. These differences and the results produced by the ORIENT model will be discussed below.

Both the Muenter model and that used by the ORIENT program employ distributed multipole moments (DMMs) to model the electrostatic part of the intermolecular interaction. The Muenter DMMs are listed in his paper; those used for the current work were calculated using the CADPAC suite of programs and are shown in Table 7.[27] They were computed through hexadecapoles at the SCF level using a TZ2P basis set from the CADPAC library.[27] The Muenter model uses a sum

**TABLE 4: Dipole Moment Components for HCCH·$N_2O$ from Experiment and Semiempirical Modeling**

| | experiment | experimental projections[a] | ORIENT (no induction, $K = 0.001225E_h$) | ORIENT (induction $K = 0.00135E_h$)[b] | ORIENT (dist. pol., $K = 0.00128E_h$)[c] |
|---|---|---|---|---|---|
| $\mu_a$/D | 0.0915(7) | 0.01 | 0.01 | 0.29 | 0.09 |
| $\mu_b$/D | 0.150(2) | 0.16 | 0.69 | 0.70 | 0.66 |
| $\mu_{tot}$/D | 0.176(2) | 0.16 | 0.69 | 0.76 | 0.67 |

[a] Projection of monomer dipole moment onto principal axes of experimental structure. [b] Induction included in calculation via monomer polarizabilities. [c] Induction included in calculation via distributed polarizabilities.

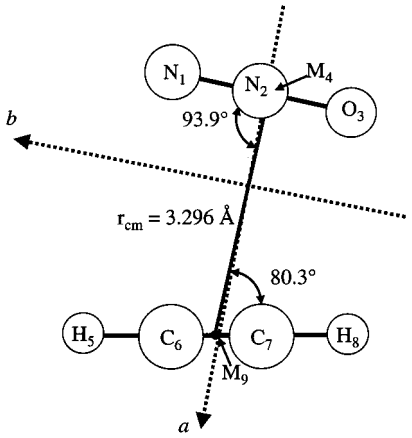


**Figure 1.** Structure of HCCH·$N_2O$ showing fitted angles and atom numbering scheme. $M_4$ and $M_9$ are the centers of mass of the two monomers.

over Lennard-Jones terms to account for the dispersion and repulsion parts of the potential, while the ORIENT model employs an exponential repulsion term, using eq 1,

$$U_{\exp-6} = \sum_{i,j} K \exp[-\alpha_{ij}(R_{ij} - \rho_{ij})] - \frac{C_6^{ij}}{R_{ij}^6} \qquad (1)$$

to describe the dispersion−repulsion part of the potential.[28] The $\alpha_{ij}$, $\rho_{ij}$, and $C_6^{ij}$ parameters in this expression have been calculated by Mirsky[29] and are listed in Table 11.2 of ref 28. $R_{ij}$ is the distance between atoms *i* and *j* on molecules *a* and *b*, respectively. The term *K* in eq 1 is a scaling factor that is adjusted to a value that reproduces the intermolecular center of mass separation well. For complexes of two linear molecules, the default value of $K = 0.001\ E_h$ ($E_h = 1$ hartree $= 27.2$ eV) is often too small, and a slightly larger value of *K* is needed to reproduce experimental distances. In this work, the values $K = 0.001225E_h$, $K = 0.00135E_h$, and $K = 0.00128E_h$ have been used to best reproduce the center of mass separation when running ORIENT with no induction, point polarizabilities, and distributed polarizabilities, respectively. The Muenter model also employs a scaling factor by which the intermolecular separation can be adjusted. This factor multiplies the van der Waals radius of each atom and is chosen to best reproduce experimental results for a specific molecule in a chosen system. The sum of scaled van der Waals radii then multiplies the repulsive term of the potential. For HCCH·$N_2O$, the factor for $N_2O$ was chosen to best reproduce the center of mass distance of that complex, and that of HCCH reproduced the separation in $(HCCH)_2$. It was found, however, that the chosen value for $N_2O$ did not reproduce the $N_2O$ dimer structure well, so the scaling factor that is designed for one system is not necessarily applicable to others.[1]

While the Muenter model did not include induction effects in the complex, the ORIENT program can account for these effects in several ways. The simplest way is to place experimental polarizabilities at a point on each molecule (usually the center of mass). For nitrous oxide these values are $\alpha = 2.93$ Å$^3$ and $\gamma = 2.83$ Å$^3$, and for acetylene they are $\alpha = 3.36$ Å$^3$ and $\gamma = 1.75$ Å$^3$.[30,31] An iterative procedure is then carried out, with one molecule inducing moments in the other and vice-versa until convergence is achieved. A more complicated way of accounting for induction is to use distributed polarizabilities. In this case, ab initio methods are used to calculate polarizabilities at points throughout a molecule (usually placed at atom centers) and then a similar iterative procedure is followed to determine the contribution of induction to the intermolecular interaction.[28] As with the DMMs, the distributed polarizabilities were calculated using the CADPAC program with a TZ2P basis set at the SCF level.[27]

The results of various HCCH·$N_2O$ structural predictions using the ORIENT semiempirical model are given in Table 5. Dipole moment predictions for these structures are shown in Table 4. It can be seen that the predicted structures vary little with the inclusion of induction in the calculations. Variation of the pre-exponential term *K* affects mainly the intermolecular separation while changing the angular relationship within the complex very little. Comparison with the experimental structure, also shown in Table 5, indicates angles and rotational constants which are well reproduced. All of the $\theta_{N_2-M_4-M_9}$ predictions are within 2.7° of the experimental value and within 0.6° of each other. The $\theta_{M_4-M_9-C_7}$ values are predicted within 1.0° of the experiment and of each other. A small variation in *K* also leads to good reproduction of the center-of-mass distance, although the default *K* of $0.001E_h$ predicts a distance that is only 0.1 Å too small. In contrast, the predictions from Muenter's model are within 1° of a parallel structure. This difference seems to be due mainly to the DMMs that were used for the predictions. If the DMMs from Muenter are used with the ORIENT program, a structure that closely resembles that proposed by Muenter is obtained. The structural parameters for this prediction are given in the last column of Table 5. Several other sets of DMMs calculated using different basis sets also led to a tilted structure with the ORIENT program, although this aspect was not exhaustively explored by us.

The fact that the predictions from the current work change little with the addition of induction to the calculation indicates that the usual procedure of neglecting induction completely is a good approximation for semiempirical modeling of this system. The inclusion of induction does become important in the prediction of dipole moment components, however. Examination of Table 4 shows that the projection of the $N_2O$ dipole moment onto the principal axes of the complex leads to a very small $\mu_a$ (~0.01 D). The experimentally determined dipole moment gave $\mu_a = 0.09$ D, however, indicating that there is an induced dipole along the *a* axis of the complex. This axis, as shown in Figure 1, connects the slightly positive central nitrogen of $N_2O$ to the $\pi$-system of the acetylene triple bond and a fair amount of induction from this quadrupole−quadrupole interaction is not surprising. The semiempirical predictions reflect this induced moment. Since CADPAC predicts a dipole moment

**TABLE 5: Structural Parameters for the HCCH·$N_2O$ Complex; See Figure 1 for the Atom Numbers**

| | experiment[a] | ORIENT $K = 0.001E_h$[b] | ORIENT $K = 0.001225E_h$[b] | ORIENT $K = 0.00135E_h$ induction[c] | ORIENT $K = 0.00128E_h$ dist. pol.[d] | previous experimental structure[e] | Muenter model[f] | ORIENT $K = 0.001E_h$ Muenter DMM[g] |
|---|---|---|---|---|---|---|---|---|
| $M_4-M_9$/Å | 3.2961(8) | 3.191 | 3.301 | 3.309 | 3.302 | 3.305 | 3.31 | 3.207 |
| $N_2-M_4-M_9$/° | 93.9(5) | 91.5 | 91.6 | 91.2 | 91.8 | 90.0 | 91 | 91.6 |
| $M_4-M_9-C_7$/° | 80.3(8) | 80.3 | 80.3 | 79.6 | 79.3 | 90.0 | 90 | 89.8 |
| *A*/MHz | 9394.2683 | 9357.9 | 9368.7 | 9359.0 | 9375.1 | 9281.2 | 9387(1) | 9320.6 |
| *B*/MHz | 2831.8564 | 3027.9 | 2828.3 | 2816.1 | 2827.0 | 2829.9 | 2829.6(3) | 3005.2 |
| *C*/MHz | 2168.0780 | 2287.7 | 2172.5 | 2164.8 | 2172.0 | 2168.7 | 2166.6(2) | 2272.5 |

[a] The quality of the fit was $\Delta I_{rms} = 0.107$ amu Å$^2$ where $\Delta I_x = I_x(\text{obs}) - I_x(\text{calc})$. [b] ORIENT model without induction, pre-exponential factor *K* as indicated. [c] ORIENT model, induction included using monomer polarizabilities, pre-exponential factor *K* as indicated. [d] ORIENT model, induction included using distributed polarizabilities, pre-exponential factor *K* as indicated. [e] Reference 2. The distance is an average distance while the angles are taken to be equilibrium values. Rotational constants were calculated from structural parameters with monomer structures from refs 23 and 24. [f] References 1 and 4. [g] ORIENT model using DMMs from reference 1.

**TABLE 6: Principal Axis Coordinates for HCCH·$N_2O$ for Tilted Structure (I) and Parallel Structure (II),[a] with Kraitchman Coordinates[b] Given in Brackets**

| | *a*/Å | | *b*/Å | |
|---|---|---|---|---|
| | I | II | I | II |
| $N_1$ | −1.311 | −1.056 | 1.194 | 1.241 |
| | [1.217] | | [1.209] | |
| $N_2$ | −1.230 | −1.214 | 0.071 | 0.126 |
| | [1.218] | | [0.065] | |
| $O_3$ | −1.145 | −1.382 | −1.117 | −1.053 |
| $M_4$ | −1.225 | −1.225 | −0.004 | 0.052 |
| $H_5$ | 2.346 | 2.306 | 1.646 | 1.557 |
| $C_6$ | 2.171 | 2.156 | 0.600 | 0.507 |
| | [2.117] | | [0.586] | |
| $C_7$ | 1.972 | 1.987 | −0.587 | −0.684 |
| | [1.992] | | [0.612] | |
| $H_8$ | 1.796 | 1.837 | −1.633 | −1.734 |
| | [1.798] | | [1.653] | |
| $M_9$ | 2.071 | 2.071 | 0.006 | −0.089 |

[a] Structures I and II were obtained from least-squares fitting $I_a$ and $I_b$ for the six isotopes; see text. [b] Coordinates calculated using Kraitchman equations (ref 25).

**TABLE 7: Distributed Multipole Moments for Acetylene and $N_2O$[a]**

| atom | coordinate[b] | $Q_{00}$ | $Q_{10}$ | $Q_{20}$ | $Q_{30}$ | $Q_{40}$ |
|---|---|---|---|---|---|---|
| H | 3.14167 | 0.03324 | 0.30454 | −0.13257 | 0.06960 | −0.04614 |
| C | 1.13667 | −0.03324 | 0.42291 | −0.30230 | −1.60327 | 2.11596 |
| C | −1.13667 | −0.03324 | −0.42291 | −0.30230 | 1.60327 | 2.11596 |
| H | −3.14167 | 0.03324 | −0.30454 | −0.13257 | −0.06960 | −0.04614 |
| N | 0.00000 | 0.62601 | 0.45467 | 0.02398 | −0.51785 | 2.39121 |
| N | −2.12783 | −0.13493 | 0.08786 | −0.06568 | 0.36881 | 0.92793 |
| O | 2.25066 | −0.49109 | 0.00439 | 0.49616 | 0.37222 | −0.73513 |

[a] All quantities are in atomic units. [b] *z* coordinate of atom in bohr.

for $N_2O$ of about 0.7 D, comparison of dipole moment predictions for different calculations should be made with some caution. It has been shown that the dipole moment of $N_2O$ is very sensitive to the level of calculation used to compute it,[32] and changes in dipole moments, indicating the direction that induced moments occur, are presumably more reliable than their magnitudes. The semiempirical calculation that neglected induction led to a very small $\mu_a$ component, just as was predicted by projection of the $N_2O$ dipole onto the experimental structure, but when induction was added to the calculation, $\mu_a$ was predicted to be significant. While the calculation that used point polarizabilities significantly overestimated the size of the induced dipole ($\mu_a \approx 0.29$ D), the distributed polarizability calculation predicted a value ($\mu_a \approx 0.09$ D) very close to the experimental one. This quantitative agreement is probably fortuitous, since ab initio dipole moment calculations usually differ significantly from experimental ones, and $\mu_b$ and the dipole moment of $N_2O$ are both overestimated by a large amount in the present calculations.

## Summary

The structure and dipole moment of the acetylene−nitrous oxide complex have been determined. The addition of isotopic data to the existing microwave data on the normal species allowed a fit of the three structural parameters to 12 moments of inertia, and substitution coordinates for five atoms were also obtained. Both the inertial fit data and the substitution coordinates indicate a structure in which the oxygen of the $N_2O$ inclines toward the acetylene with an angle between the monomers of 13.6°. This structure agrees very well with that predicted using a semiempirical model that employs distributed multipole analyses to model the electrostatic interaction and analytic dispersion and repulsion terms. Angles are predicted to within 2.5° and distances to within 0.1 Å when using default parameters. The use of experimental monomer polarizabilities and ab initio distributed polarizabilities did not change the predicted structure significantly from calculations that neglected induction effects. The change in the predicted $\mu_a$ dipole moment upon addition of induction to the calculation was in the direction expected based on the experimental results.

The slightly tilted $N_2O$ structure determined in this work differs from an interaction model described by Muenter and previously used on the $(HCCH)_2$, HCCH·$CO_2$ and $(CO_2)_2$ complexes.[1,4] The differences in predicted structures can be attributed to the different DMMs in the Muenter model compared to the ORIENT model. The ORIENT semiempirical model has worked well on many other dimers and trimers of linear molecules, including HCCH·OCS,[7] HCCH$(OCS)_2$,[8] $(OCS)_2CO_2$,[11] $CO_2$·OCS,[9] and $(CO_2)_2N_2O$,[12] so it seems unlikely that its agreement with the experimental structure of HCCH·$N_2O$ is purely fortuitous. Nevertheless, the ORIENT semiempirical model and the Muenter model are quite simplistic, and close agreement (or disagreement) with experimental details should not be considered profoundly significant. Furthermore, the difference between the parallel and tilted structures is quite small and subtle. Given the nonrigidity of such complexes, a rigorous determination of the equilibrium structure must await further experimental and theoretical developments. Equilibrium configurations much closer to parallel cannot be completely eliminated with the present data.

**Acknowledgment.** R.A.P, S.A.P., and R.L.K thank the National Science Foundation Experimental Physical Chemistry Program for funding and Dr. Anthony Stone for his kind assistance with distributed polarizability calculations in ORIENT

and CADPAC. H.O.L acknowledges the donors of the Petroleum Research Fund, administered by the American Chemical Society, a Cottrell College Science Award of Research Corporation, the National Science Foundation (CHE-9727382), and the Henry Dreyfus Teacher-Scholar Awards Program for support of this research.

## References and Notes

(1) Hu, T. A.; Sun, L. H.; Muenter, J. S. *J. Chem. Phys.* **1991**, *95*, 1537.
(2) Leung, H. O. *J. Chem. Phys.* **1997**, *107*, 2232.
(3) Leung, H. O. *Chem. Commun.* **1996**, *22*, 2525.
(4) Muenter, J. S. *J. Chem. Phys.* **1991**, *94*, 2781.
(5) Muenter, J. S. *J. Chem. Phys.* **1989**, *90*, 4048.
(6) Prichard, D. G.; Nandi, R. N.; Muenter, J. S.; Howard, B. J. *J. Chem. Phys.* **1988**, *89*, 1245.
(7) Peebles, S. A.; Kuczkowski, R. L. *J. Phys. Chem.* **1999**, *103*, 3884.
(8) Peebles, S. A.; Kuczkowski, R. L *Chem. Phys. Lett.* **1999**, *308*, 21.
(9) Peebles, S. A.; Kuczkowski, R. L. *J. Chem. Phys.* **1998**, *109*, 5276.
(10) Peebles, S. A.; Kuczkowski, R. L. *Chem. Phys. Lett.* **1998**, *286*, 421.
(11) Peebles, S. A.; Kuczkowski, R. L. *J. Phys. Chem.* **1998**, *102*, 8091.
(12) Peebles, R. A.; Peebles, S. A.; Kuczkowski, R. L. *Mol. Phys.* **1999**, *96*, 1355.
(13) Block, P. A.; Marshall, M. D.; Pedersen, L. G.; Miller, R. E. *J. Chem. Phys.* **1992**, *96*, 7321.
(14) Peterson, K. I.; Klemperer, W. *J. Chem. Phys.* **1984**, *80*, 2439.
(15) Zolandz, D.; Yaron, D.; Peterson, K. I.; Klemperer, W. *J. Chem Phys.* **1992**, *97*, 2861.
(16) Balle, T. J.; Flygare, W. H. *Rev. Sci. Instrum.* **1981**, *52*, 33.
(17) Leung, H. O.; Gangwani, D.; Grabow, J.-U. *J. Mol. Spectrosc.* **1997**, *184*, 106.
(18) Hillig, K. W., II; Matos, J.; Scioly, A.; Kuczkowski, R. L. *Chem. Phys. Lett.* **1987**, *133*, 359.
(19) Tubergen, M. J.; Kuczkowski, R. L. *J. Mol. Struct.* **1995**, *352/353*, 335.
(20) Muenter, J. S. *J. Chem. Phys.* **1968**, *48*, 4544.
(21) Scharpen, L. H.; Muenter, J. S.; Laurie, V. W. *J. Chem. Phys.* **1970**, *53*, 2513.
(22) Fits of $I_a$ and $I_c$ gave comparable $\Delta I_{rms}$ and $\theta_{N_2-M_4-M_9} = 94.3(6)°$, $\theta_{M_4-M_9-C_7} = 80.9(9)°$, and $r_{cm} = 3.3033(6)$ Å. The values from the fit of $I_a$ and $I_b$ are slightly preferred since $\Delta I_{rms}$ is marginally smaller. Fits of $I_b$ and $I_c$ would not converge.
(23) Coles, D. K.; Elyash, E. S.; Gorman, U. J. G. *Phys. Rev.* **1947**, *72*, 9732.
(24) Harmony, M. D.; Laurie, V. W.; Kuczkowski, R. L.; Schwendeman, R. H.; Ramsay, D. A.; Lovas, F. J.; Lafferty, W. J.; Maki, A. G. *J. Phys. Chem. Ref. Data* **1979**, *8*, 619.
(25) Kraitchman, J. *Am. J. Phys.* **1953**, *21*, 17.
(26) Stone, A. J.; Dullweber, A.; Hodges, M. P.; Popelier, P. L. A.; Wales, D. J. *ORIENT: A program for studying interactions between molecules*, version 3.2; University of Cambridge, 1995.
(27) *CADPAC: The Cambridge Analytic Derivatives Package*, issue 6; Cambridge, 1995. A suite of quantum chemistry programs developed by Amos, R. D. with contributions from Alberts, I. L.; Andrews, J. S.; Colwell, S. M.; Handy, N. C.; Jayatilaka, D.; Knowles, P. J.; Kobayashi, R.; Laidig, K. E.; Laming, G.; Lee, A. M.; Maslen, P. E.; Murray, C. W.; Rice, J. E.; Simandiras, E. D.; Stone, A. J.; Su, M.-D.; Tozer, D. J.
(28) Stone, A. J. *The Theory of Intermolecular Forces*; Clarendon Press: Oxford, 1996.
(29) Mirsky, K. In *The Determination of Intermolecular Interaction Energy By Empirical Methods*; Schenk, R., Olthof-Hazenkamp, R., Van Koningveld, H., Bassi, G. C., Eds.; Delft University Press: Delft, The Netherlands, 1978.
(30) Alms, G. R.; Burnham, A. K.; Flygare, W. H. *J. Chem. Phys.* **1975**, *63*, 3321.
(31) Gray, C. G.; Gubbins, K. E. *Theory of Molecular Fluids Vol. 1: Fundamentals*; Oxford University Press: Oxford, 1984.
(32) Mogi, K.; Komine, T.; Hirao, K. *J. Chem. Phys.* **1991**, *95*, 8999.